A Brief Introduction to Medical Imaging

Outline

- General Goals
- Linear Imaging Systems
- An Example, The Pin Hole Camera
- Radiations and Their Interactions with Matter
- Coherent vs. Incoherent Imaging
- Length Scales
- Contrasts
- Photon Intensity Tomography
- Magnetic Resonance Imaging

Imaging Definitions

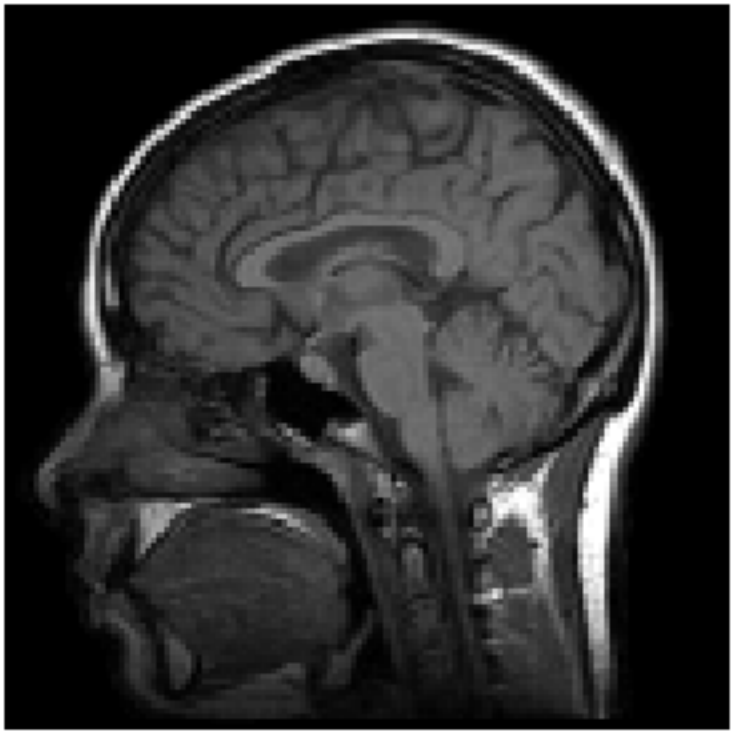

Object function - the real space description of the actual object.

Resolution - the collected image is only an approximation of the actual object. The resolution describes how accurate the spatial mapping is?

Distortions - describes any important non-linearities in the image. If there are no distortions, then the resolution is the same everywhere.

Fuzziness - describes how well we have described the object we wish to image.

Contrast - describes how clearly we can differentiate various parts of the object in the image.

Signal to Noise ratio

Linear Imaging Systems

If the blurring of the object function that is introduced by the imaging processes is spatially uniform, then the **image** may be described as a **linear** mapping of the **object function.**

This mapping is, of course, at lower resolution; and the blurring is readily described as a **convolution** of the object function with a ***Point Spread Function***.

$$\text{Image} = \text{object} \otimes \text{Point Spread Function} + \text{noise}$$

The noise is an important consideration since it limits the usefulness of deconvolution procedures aimed at reversing the blurring effects of the image measurement.

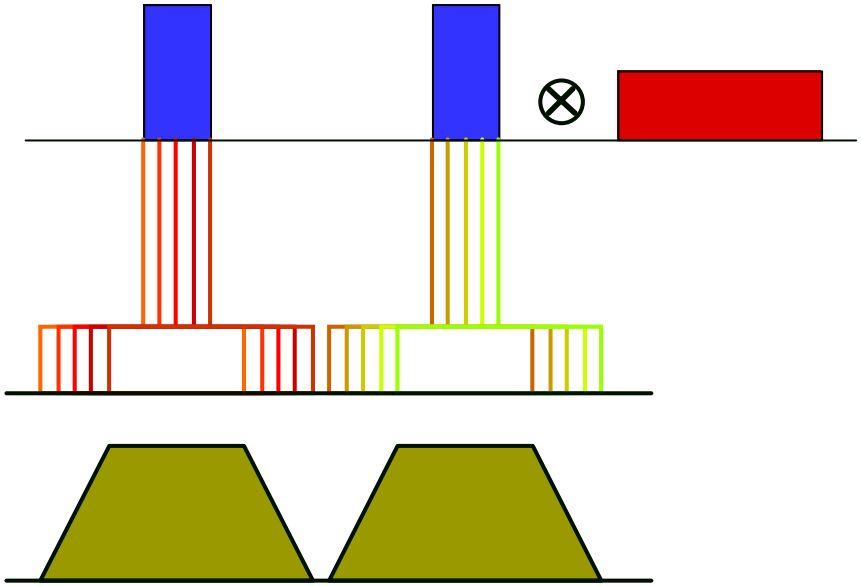

An Example, the Pin-hole Camera

One of the most familiar imaging devices is a pin-hole camera.

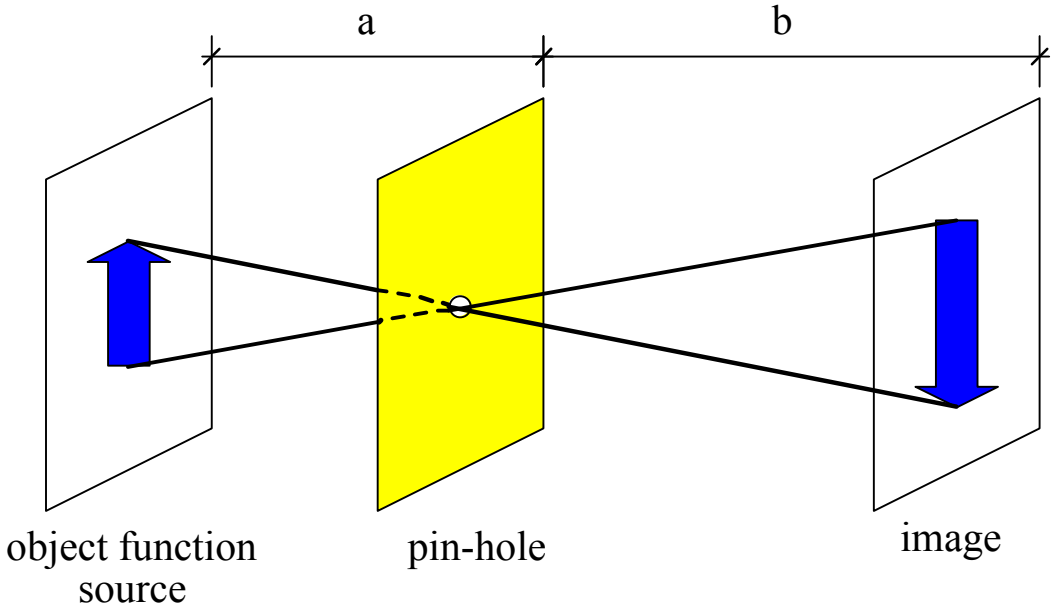

The object is magnified and inverted. Magnification = -b/a.

An Example, the Pin-hole Camera 2

Notice, however, that the object function is also blurred due to the finite width of the pin-hole.

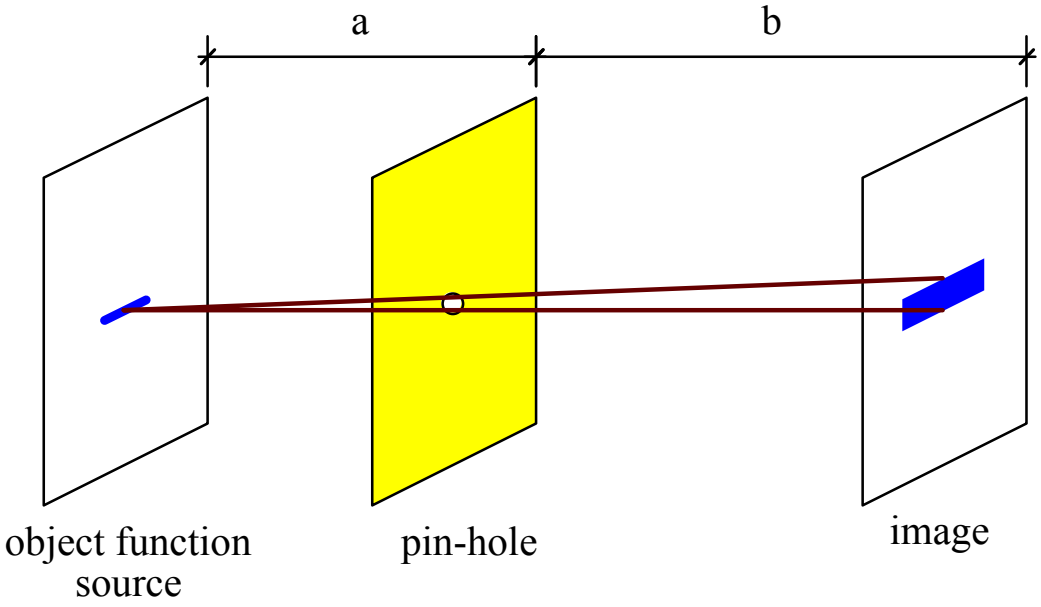

The extent of blurring is to multiply each element of the source by the "source magnification factor" of (a+b)/a x diameter of the pin-hole.

Distortions of a Pin-hole Camera

Even as simple a device as the pin-hole camera has distortions
1. Limited field of view due to the finite thickness of the screen.

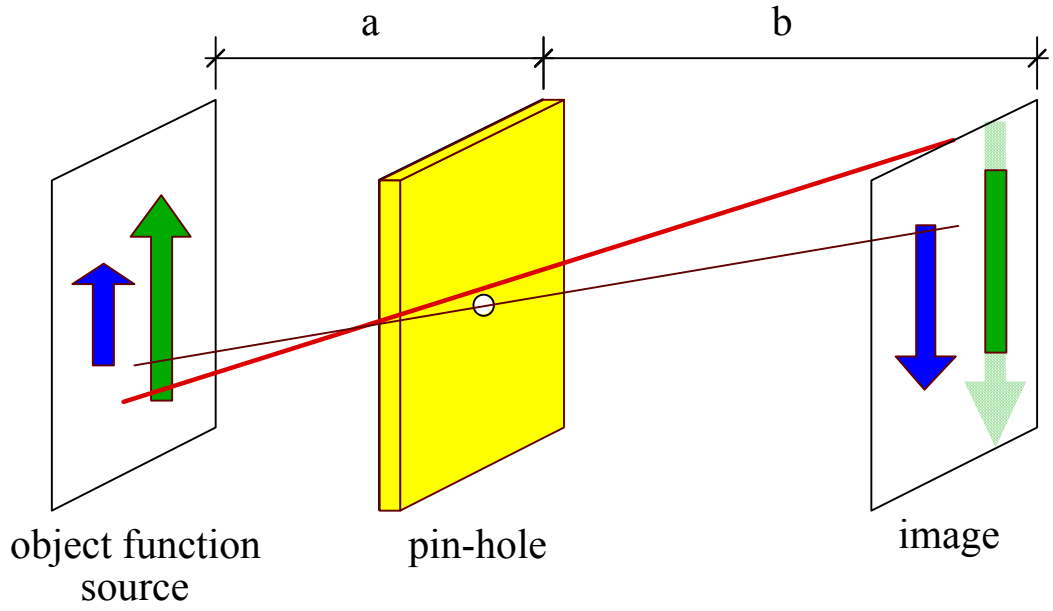

As the object becomes too large, the ray approaches the pin-hole too steeply to make it through.

Distortions of a Pin-hole Camera 2

Also, as the object moves off the center line, the shadow on the detector grows in area, (and the solid angle is decreased) so the image intensity is reduced.

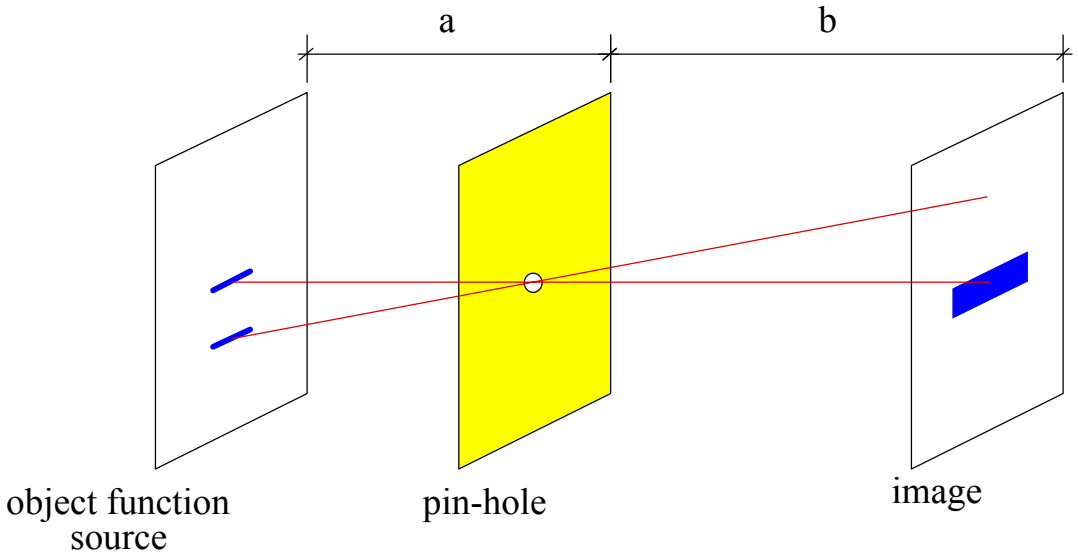

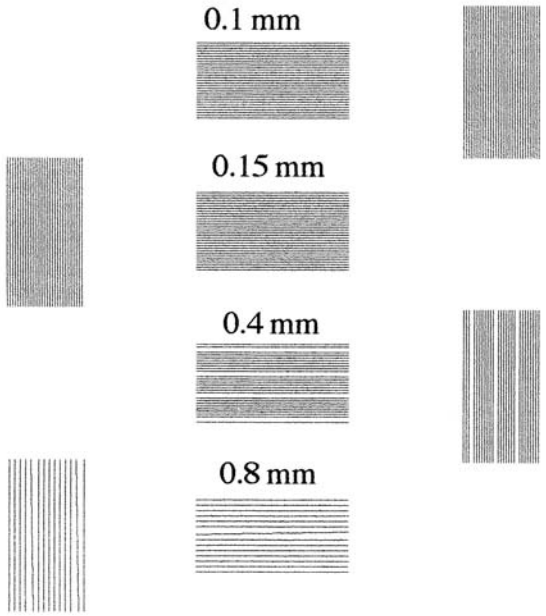

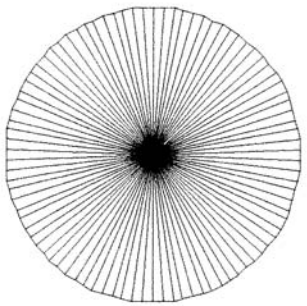

4°

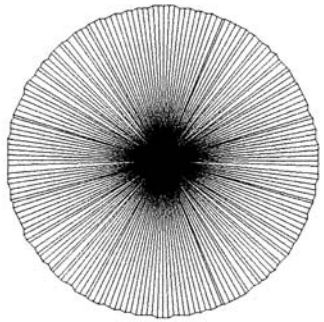

2°

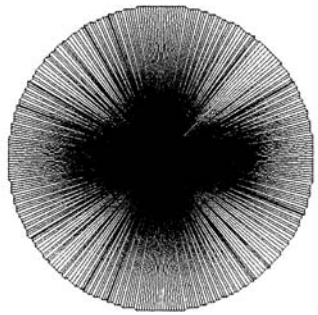

1°

Spatial Frequencies

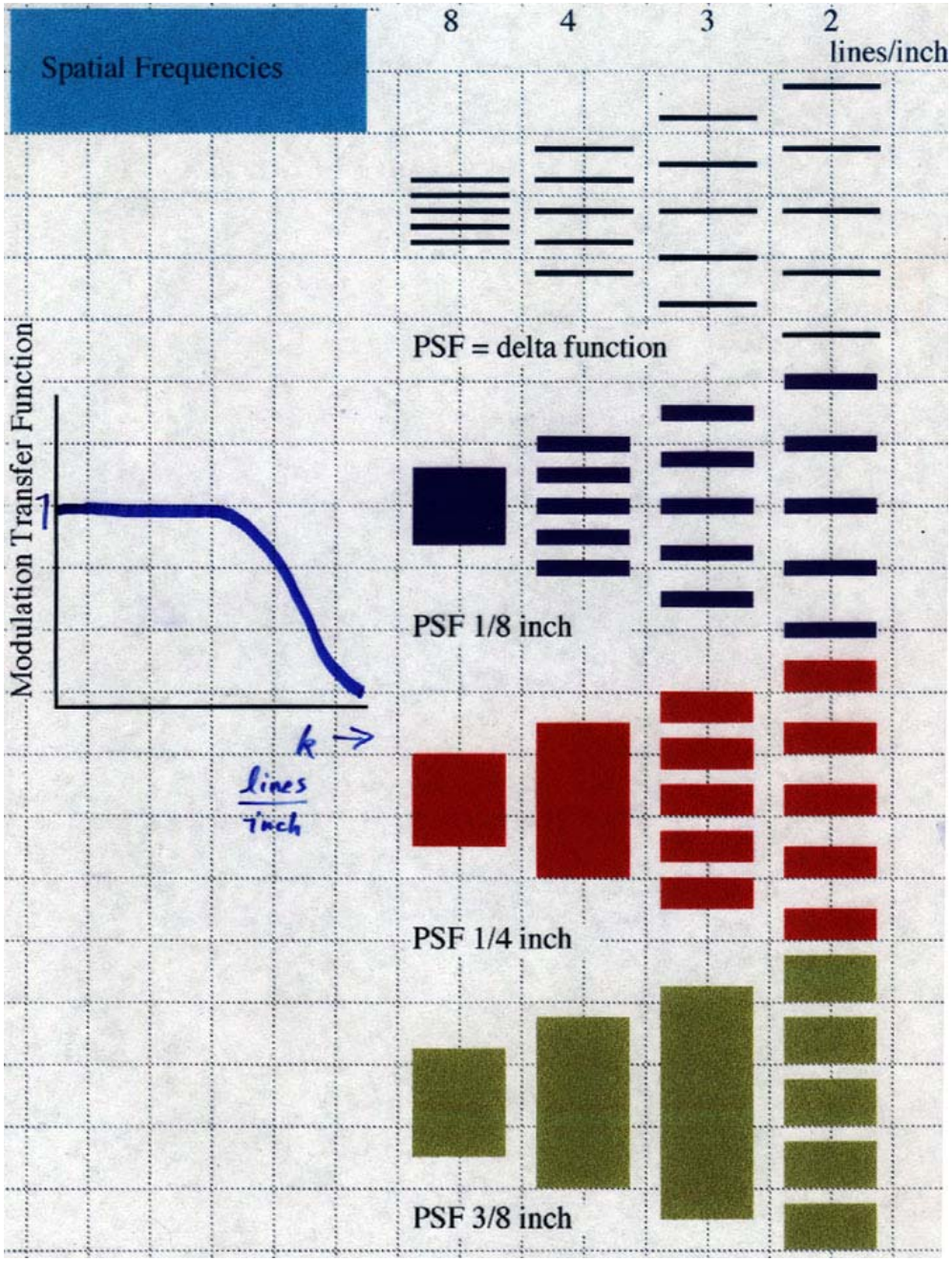

Spatial Frequencies 2

When discussing linear imaging systems it is often useful to describe the measurement in terms of a mapping of Fourier components of the object function.

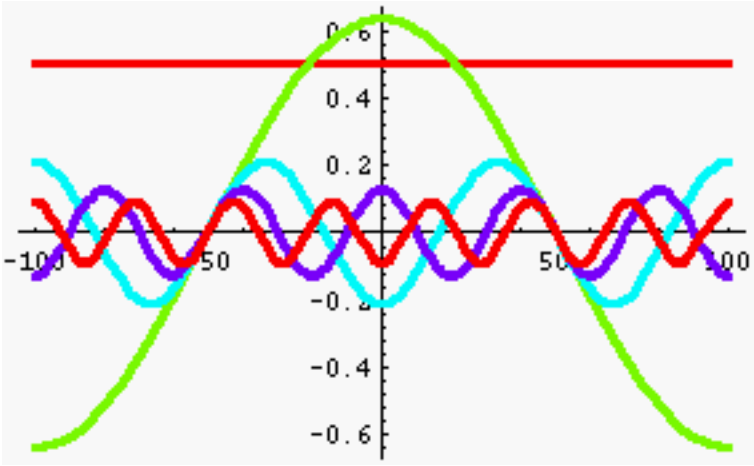

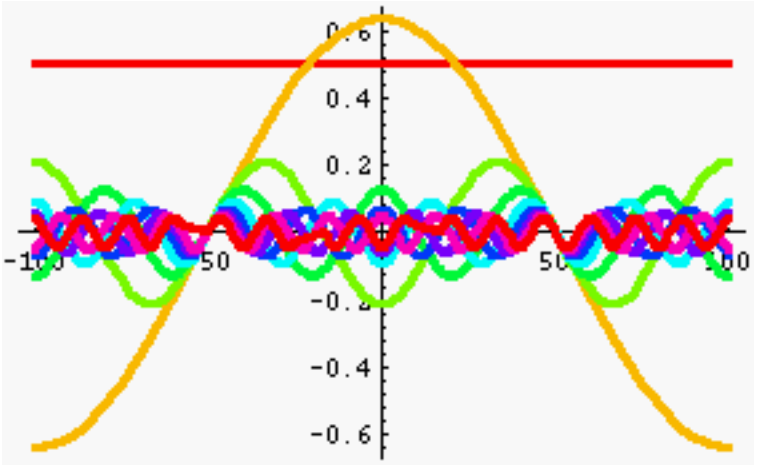

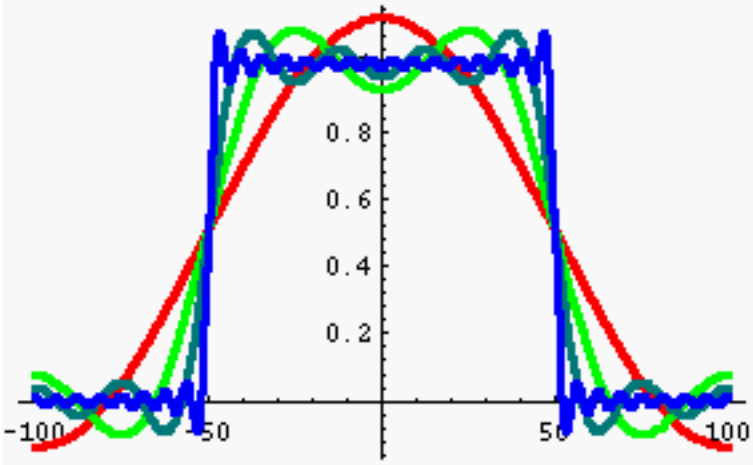

Transmission Tomography

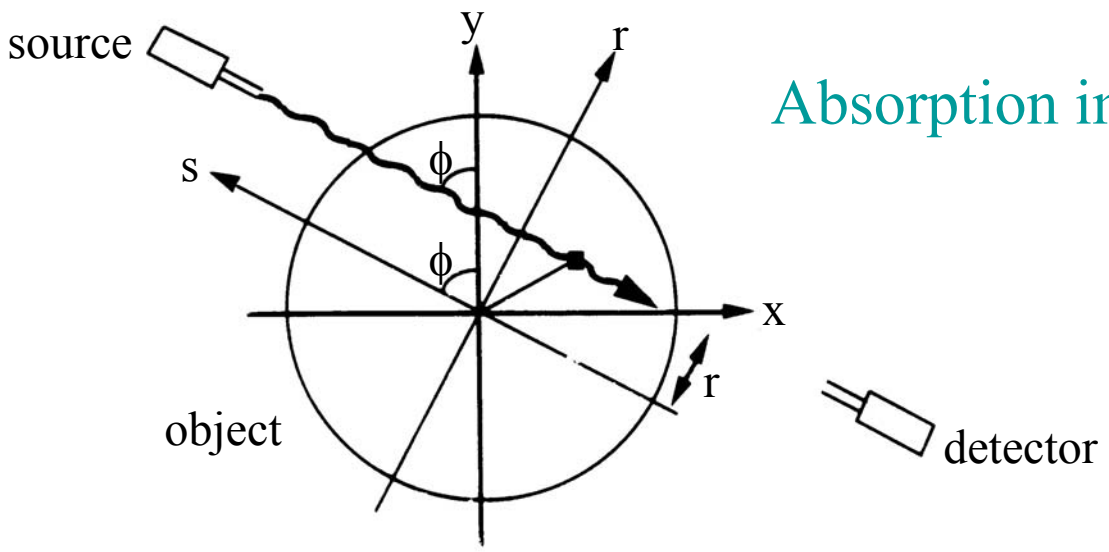

Absorption imaging

In absorption imaging, the integrated absorption along a column through the object is measured. An array of detectors therefore measures a ‘shadow profile’.

Projection Imaging

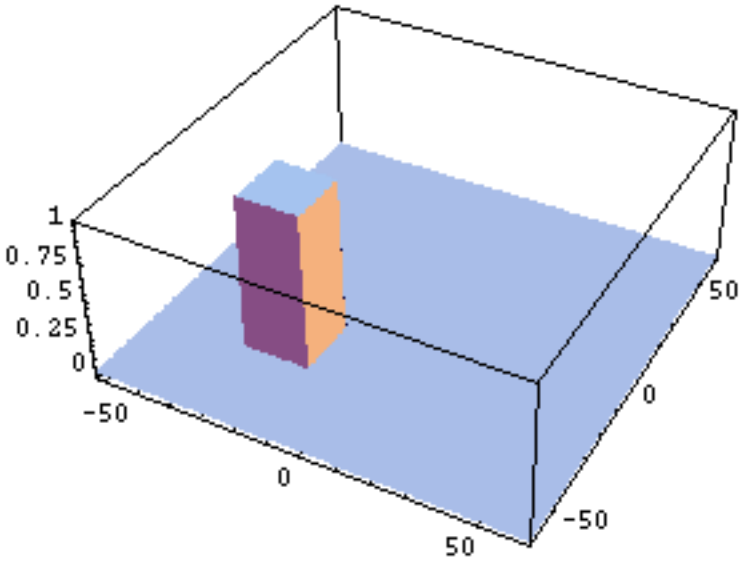

Object

Projections

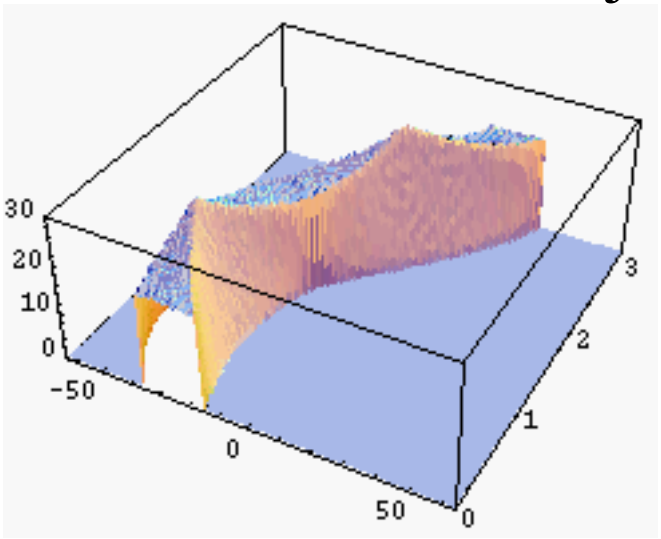

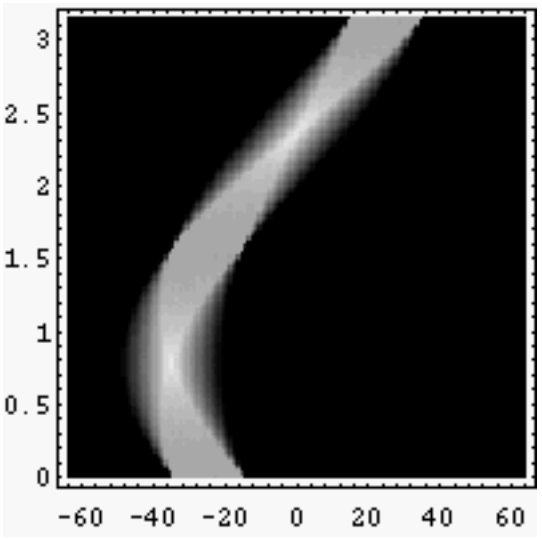

Central Slice Theorem

Consider a 2-dimensional example of an emission imaging system. **O(x,y)** is the **object function**, describing the source distribution. The projection data, is the line integral along the projection direction.

$$P(0^\circ, y) = \int O(x,y)\,dx$$

The central slice theorem can be seen as a consequence of the separability of a 2-D Fourier Transform.

$$\tilde{o}(k_x, k_y) = \int O(x,y) e^{-ik_x x} e^{-ik_y y}\,dx\,dy$$

The 1-D Transform of the projection is,

$$\begin{aligned}
\tilde{p}(k_y) &= \int P(0^\circ, y) \cdot e^{-ik_y y}\,dy \\
&= \iint O(x,y) \cdot e^{-ik_y y}\,dx\,dy \\
&= \iint O(x,y) \cdot e^{-ik_y y} \cdot e^{-i0x}\,dx\,dy \\
&= \tilde{o}(0, k_y)
\end{aligned}$$

The one-dimensional Fourier transformation of a projection obtained at an angle J, is the same as the radial slice taken through the two-dimensional Fourier domain of the object at the same angle.

Transmission Tomography

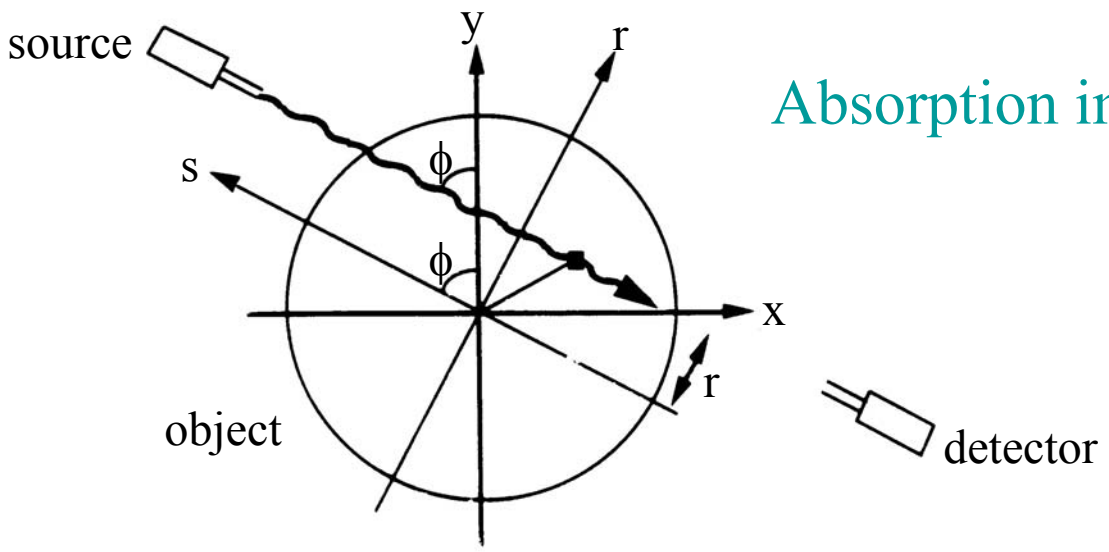

Absorption imaging

In absorption imaging, the integrated absorption along a column through the object is measured. An array of detectors therefore measures a ‘shadow profile’.

Coherent vs. Incoherent Imaging

In both cases the image is the result of the scattering of a field by the object.

Incoherent - measure only the *intensity* fluctuations of this scatter. Usually frequencies are too high to permit convenient measures of the phase. Examples,

light	10^{14} Hz
X-rays	10^{18} Hz
γ-rays	10^{20} Hz

A photograph is an incoherent image.

Coherent - measure both the *intensity* and the *phase* of the scattered field. This is usually measured as a temporal evolution of the scattered field. The frequency of radiation is normally quite low to permit an accurate measure of the phase (such as microwaves). MRI is an example of coherent imaging.

Incoherent images are most readily measured by scanning a well collimated beam across the sample and observing the attenuation of that beam (this may be multiplexed with many detectors).

Coherent images permit the characterization of the entire sample at once and with observation through a single detector element. A series of measurements are made for fields of varying frequency or direction.

X-ray Attenuation Coefficients

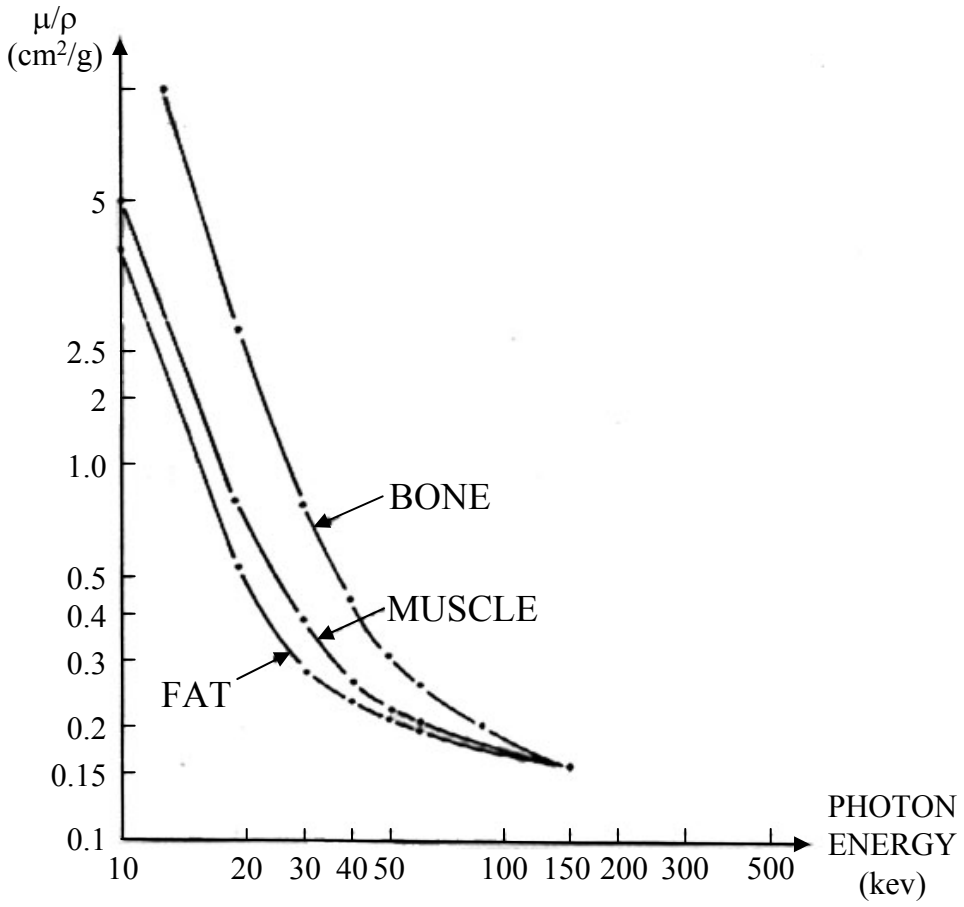

X-ray attenuation coefficients for muscle, fat, and bone, as a function of photon energy.

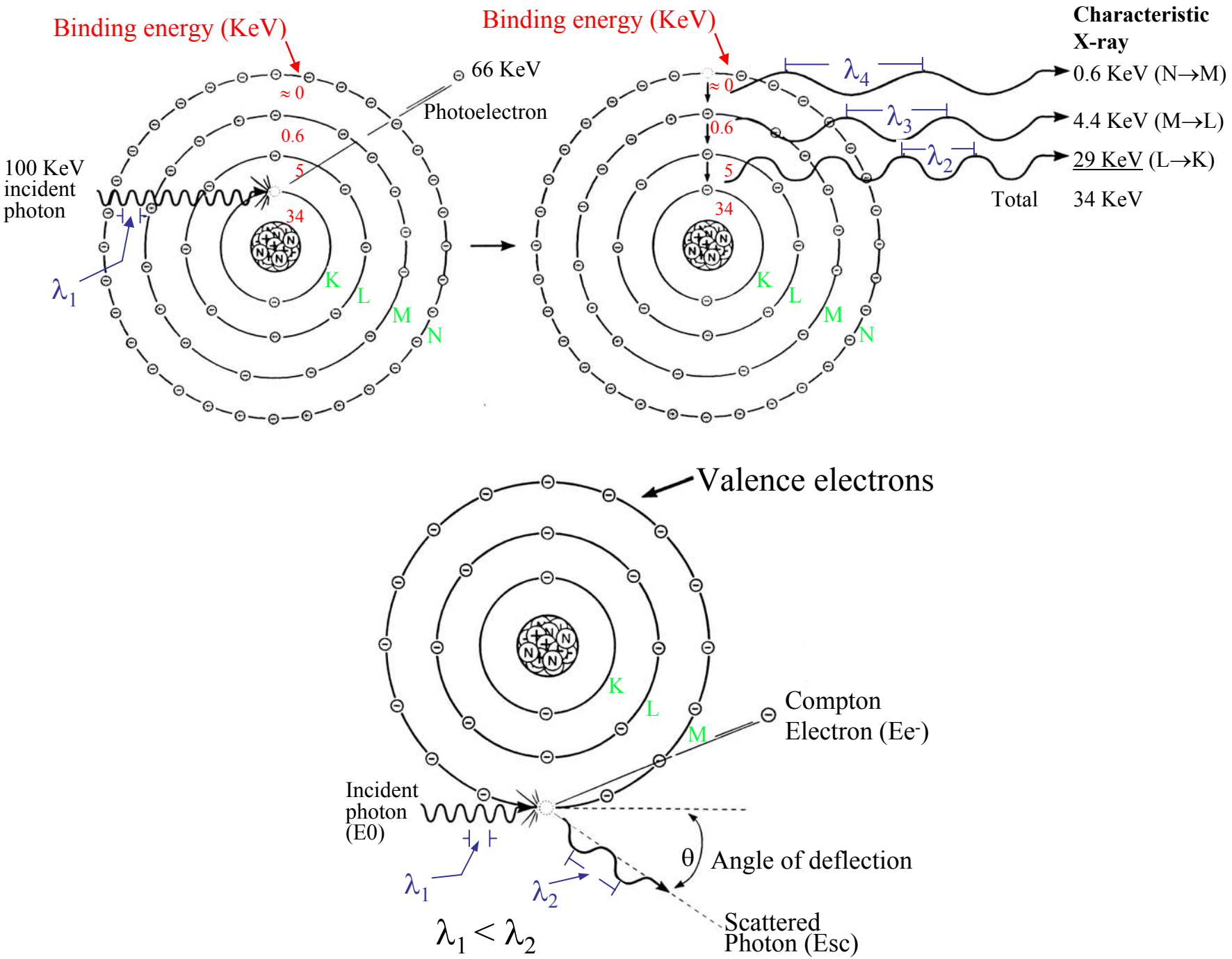
Binding energy (KeV)
≈ 0
0.6
5
34
66 KeV
Photoelectron
100 KeV
incident
photon
λ1
K
L
M
N
Binding energy (KeV)
≈ 0
0.6
5
34
λ4
λ3
λ2
Characteristic
X-ray
0.6 KeV (N→M)
4.4 KeV (M→L)
29 KeV (L→K)
Total
34 KeV
Valence electrons
K
L
M
Compton
Electron (Ee-)
Incident
photon
(E0)
λ1
λ2
θ
Angle of deflection
Scattered
Photon (Esc)
λ1 < λ2

Attenuation Mechanisms

	μ Dependence		
Mechanism	E	Z	Energy Range in Soft Tissue
Simple Scatter	$1/E$	Z^2	1-20 keV
Photoelectric	$1/E^3$	Z^3	1-30 keV
Compton	falls slowly with E	independent	30 keV-20 MeV
Pair Production	rises slowly with E	Z^2	above 20 MeV

Attenuation Mechanisms 2

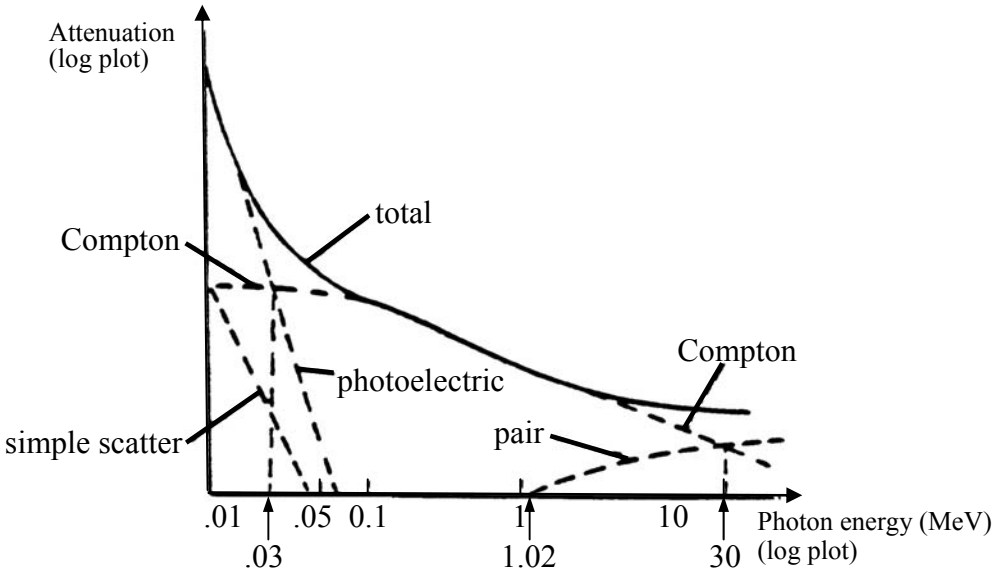

Attenuation mechanisms in water

The optimum photon energy is about 30 keV (tube voltage 80-100 kV) where the photoelectric effect dominates. The Z^3 dependence leads to good contrast:

Z_{fat}	5.9
$Z_{muscles}$	7.4
Z_{bone}	13.9

$\Rightarrow$ Photoelectric attenuation from bone is about 11x that due to soft tissue, which is dominated by Compton scattering.

Photon Intensity Tomography

	X-ray CT	SPECT	PET
measuring	X-ray attenuation	source distribution of radio-pharmaceuticals, gamma emitters	source distribution of radio-pharmaceuticals, positron emitters
anatomical information	Yes	No	No
beam definition	collimators	collimators	coincidence detection

Photon Intensity Tomography 1

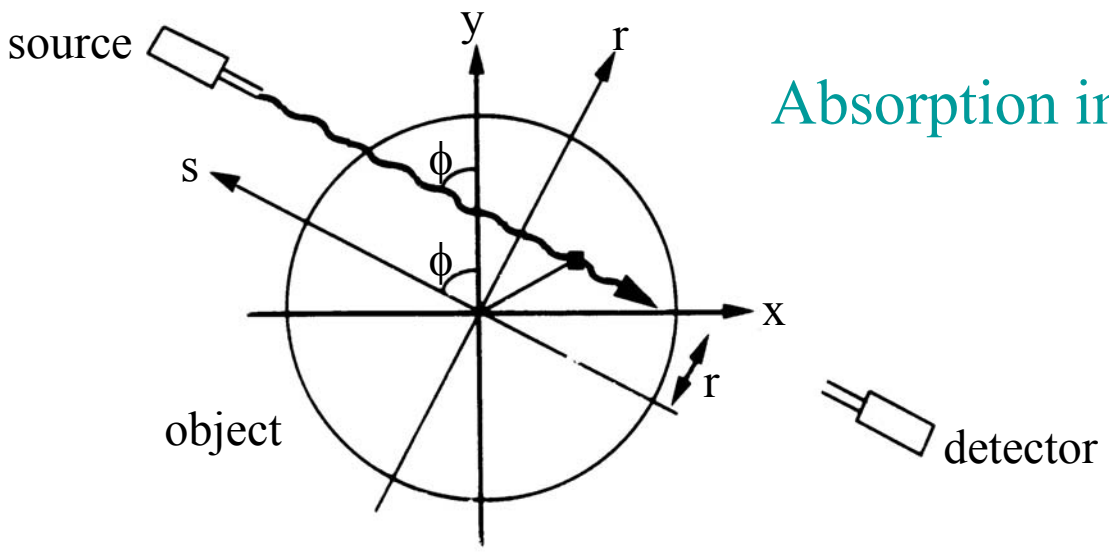

Absorption imaging

In absorption imaging, the integrated absorption along a column through the object is measured. An array of detectors therefore measures a ‘shadow profile’.

Photon Intensity Tomography 2

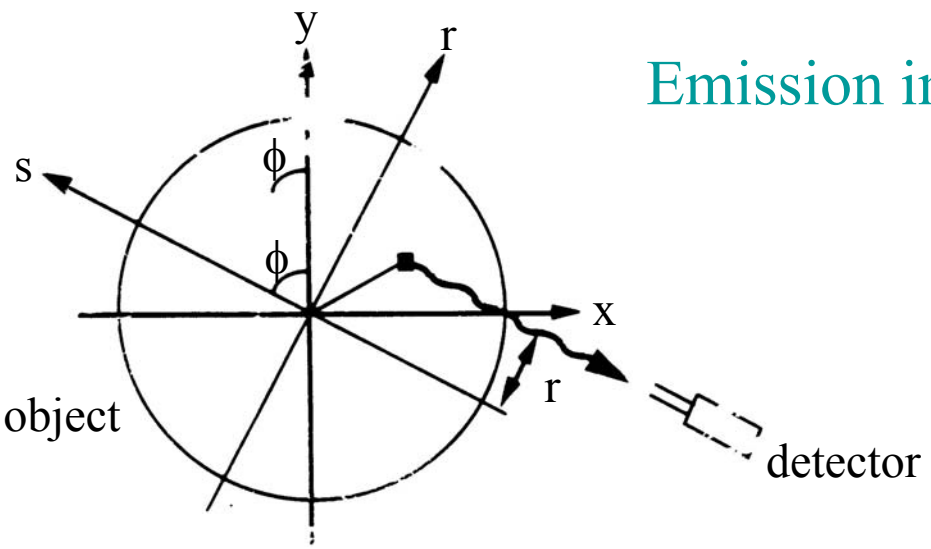

Emission imaging

In emission imaging, the integrated emitter density is measured.

Spatial and Temporal Limits in NMR

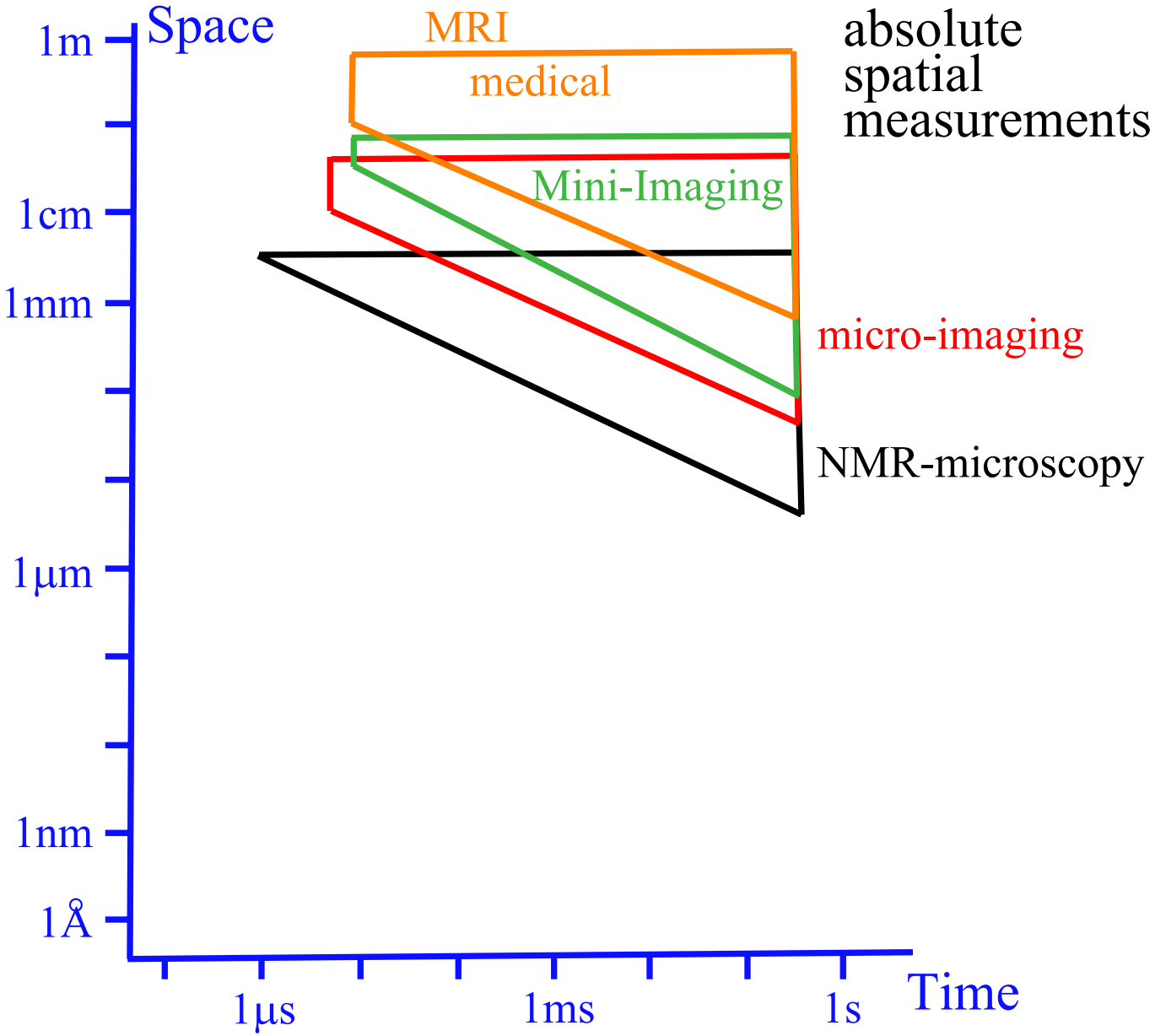

The Bloch Equations

$$\frac{d}{dt}M_x = \Delta\omega \cdot M_y - \frac{M_x}{T_2}$$

$$\frac{d}{dt}M_y = -\Delta\omega \cdot M_x + \omega_1(t) \cdot M_z - \frac{M_y}{T_2}$$

$$\frac{d}{dt}M_z = -\omega_1(t) \cdot M_y - \frac{M_z - M_0}{T_1}$$

ω_1 is the strength of an applied external resonant radio-frequency field. $\Delta\omega$ is the precession frequency; it includes contributions from

- variations in magnetic field strength (inhomogeneities),
- applied magnetic field gradients,
- chemical shifts (screening of the nucleus by surrounding electrons),
- and coupling of spins to each other (the dynamics are more complicated than indicated by the Bloch equations however).

Spin Magnetization Gratings

Grating - "a system of equidistant and parallel lines… to produce spectra by diffraction".

Spin magnetization grating - a periodic modulation of the phase (or amplitude) of the local spin magnetization vector superimposed on the spin density

Spin Magnetization gratings may be created by spin evolution in a linearly increasing magnetic field.

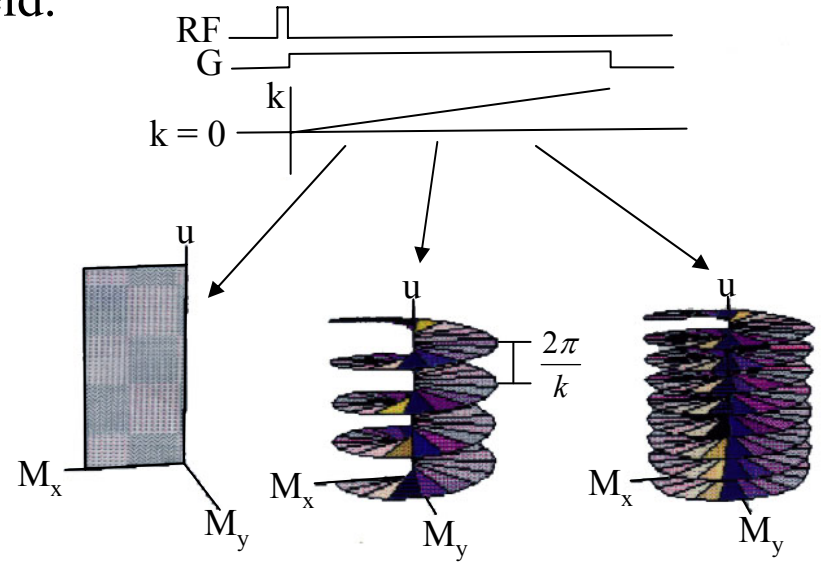

This produces a grating as a linear phase ramp, since motions are torques.

Moire complex gratings are produced through a combination of RF and gradient pulses. The spatial frequency distribution of these are describable by a distribution of components, each at a given wave-number.

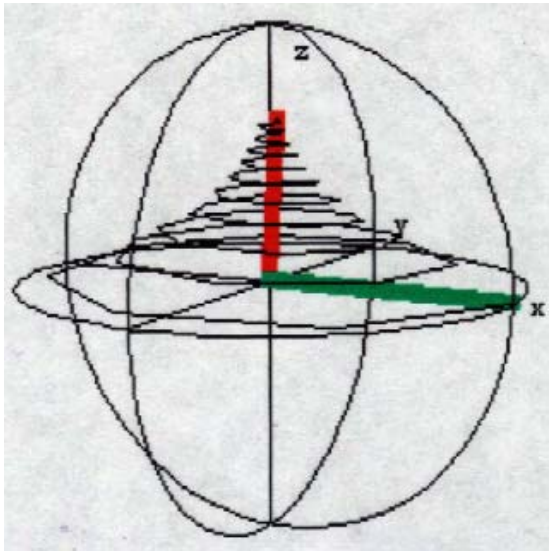
z
y
x

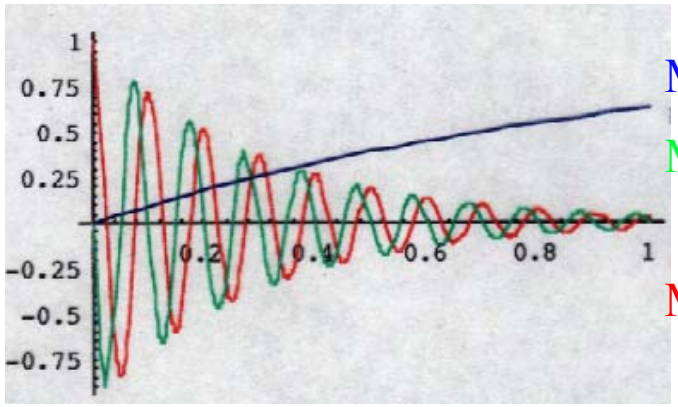
1
0.75
0.5
0.25
-0.25
-0.5
-0.75
0.2
0.4
0.6
0.8
1
$M_z(t)$
$M_y(t)$
time
$M_x(t)$

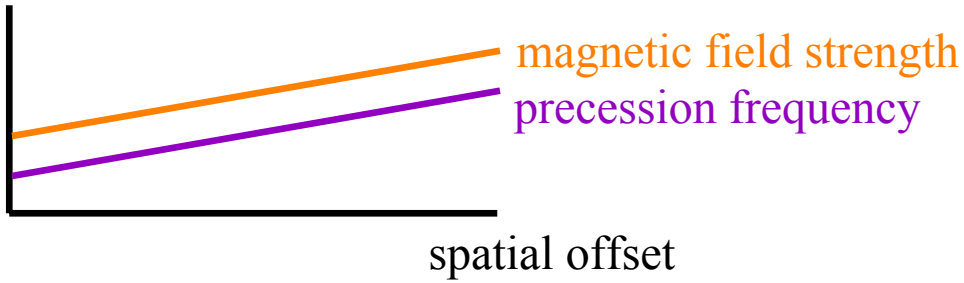
magnetic field strength
precession frequency
spatial offset

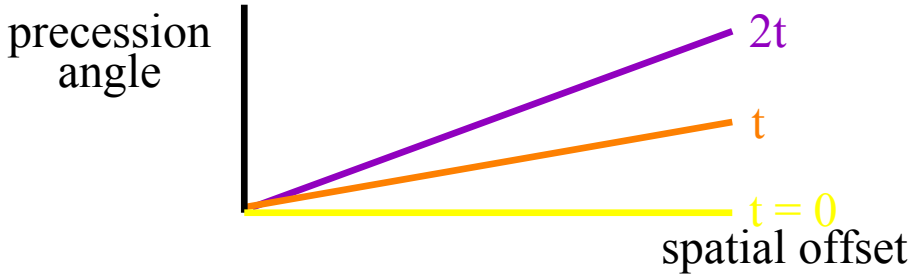
precession angle
2t
t
t = 0
spatial offset

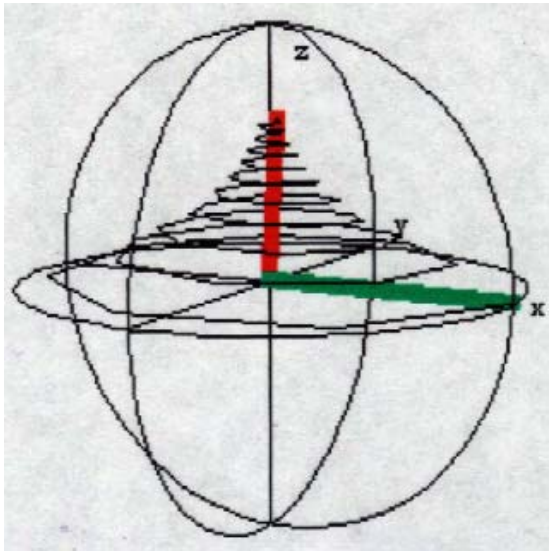

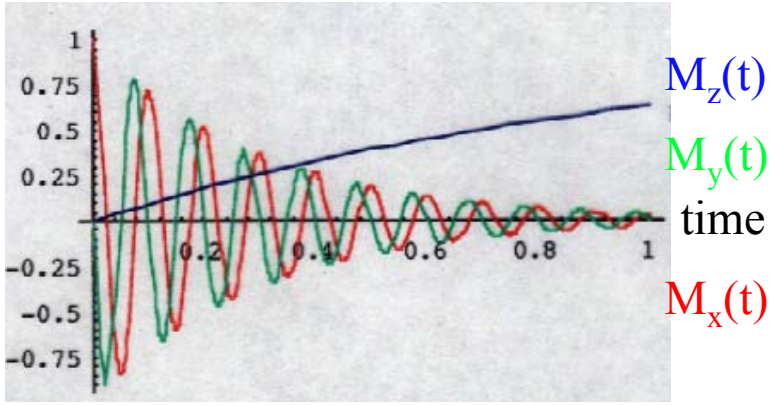

Diagrams of the spin magnetization's return to equilibrium after being aligned along the x-axis. In both pictures the evolution of a single bulk magnetization vector is being followed. The initial position is shown as the green vector at top, which spirals into the z-axis, the red vector. In the figure on the right, the three individual components of the magnetization are shown as a function of time. The NMR experiment measures the two transverse components, M_x and M_y. There are three motions, a precession about the z-axis, a decay of the transverse components and a slower growth along z towards the static equilibrium value.

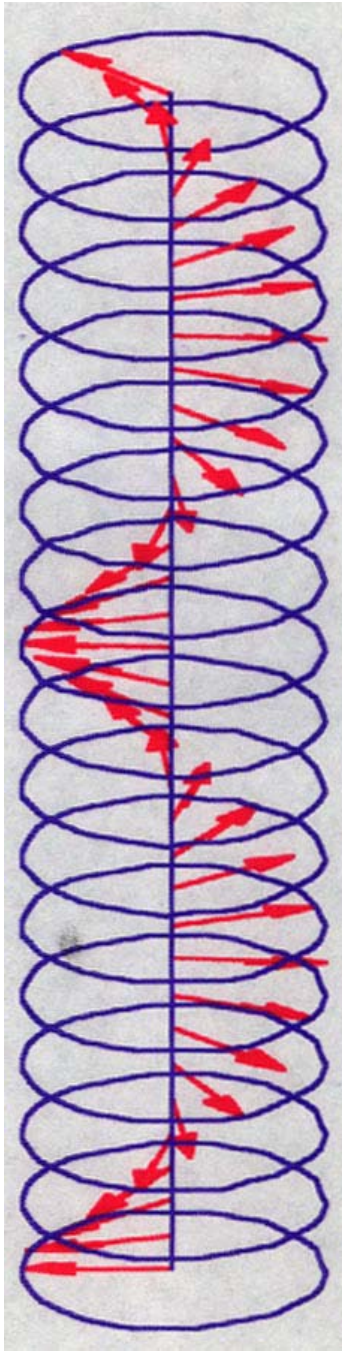

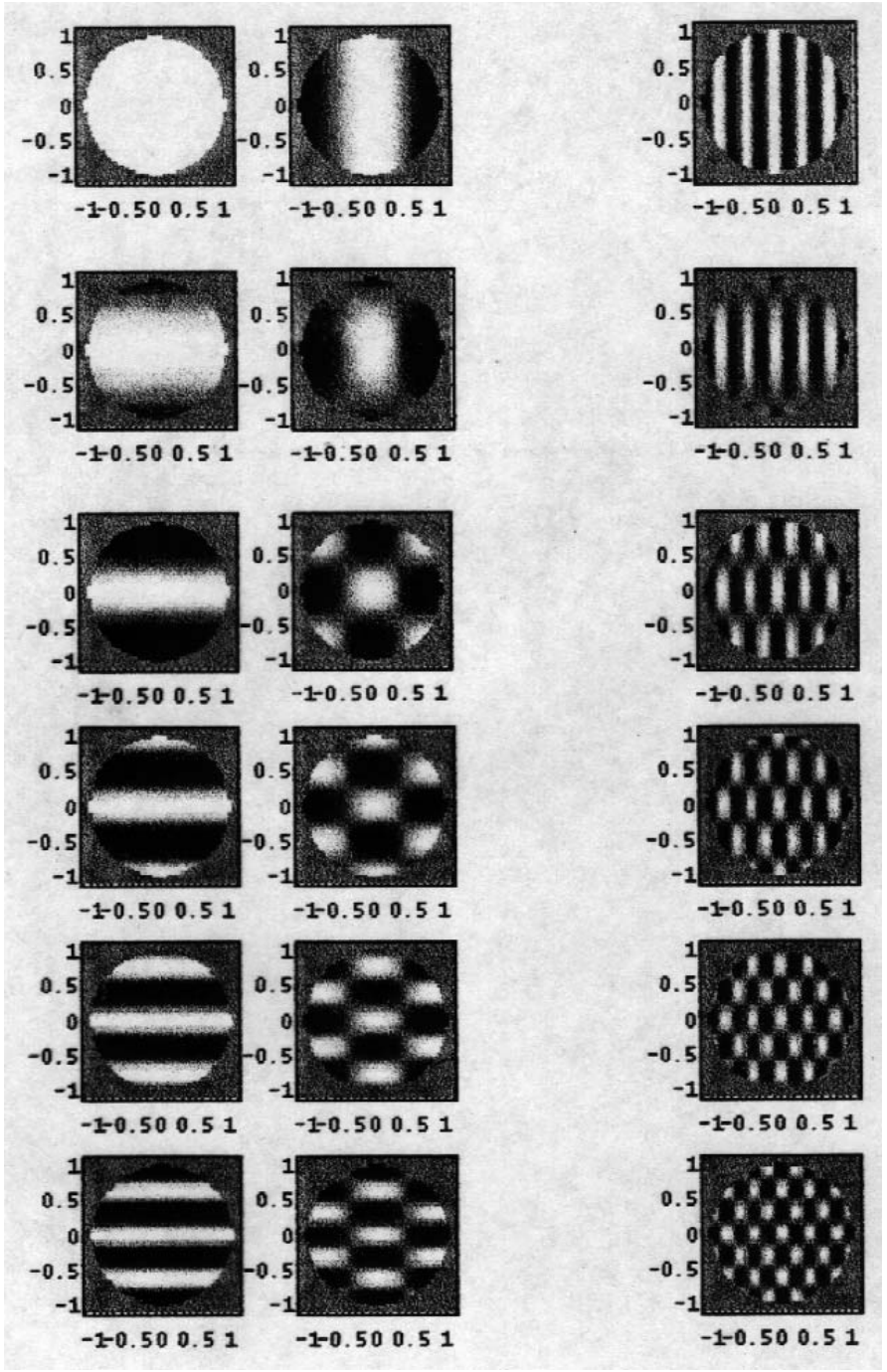
1
0.5
0
-0.5
-1
-1-0.50 0.5 1

attenuation

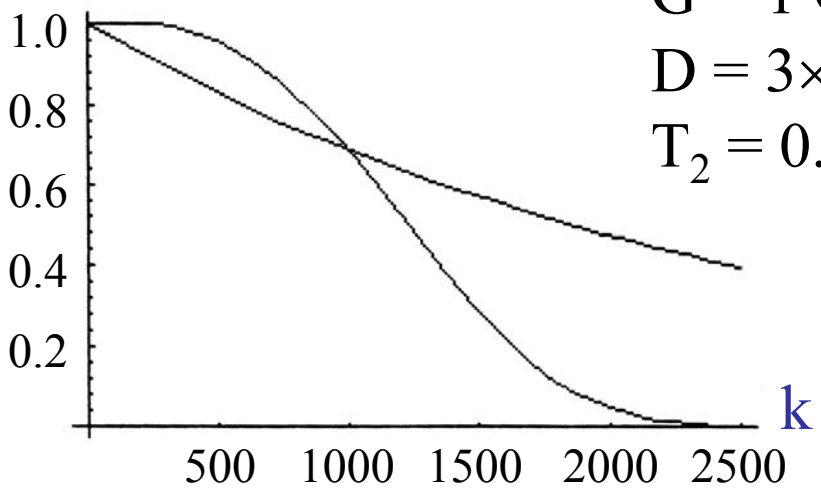

G = 1 G/cm

D = 3×10^{-5} cm^2/s

T_2 = 0.1 s

$$t = \frac{k}{\gamma G}$$

attenuation $T_2 = e^{-\frac{k}{\gamma G T_2}};\ e^{-\frac{t}{T_2}}$

attenuation $D = e^{-\frac{k^3 D}{3\gamma G}};\ e^{-\frac{k^2 D t}{3}}$